Comparison of Total Received Power and Mean Effective Gain for Mobile Handsets

Nielsen, Jesper Ødum; Pedersen, Gert F.

Publication date:
2002

Document Version
Publisher's PDF, also known as Version of record

EUROPEAN COOPERATION
IN THE FIELD OF SCIENTIFIC
AND TECHNICAL RESEARCH

EURO-COST

SOURCE: Center for PersonKommunikation,
Aalborg University

COST 273 TD(02) 021
Guildford, UK
January 17–18, 2002

Comparison of Total Received Power and Mean Effective Gain for Mobile Handsets

Jesper Ødum Nielsen, Gert Frølund Pedersen
Niels Jernes Vej 12
9220 Aalborg Ø
Denmark
Phone: +45 9635 8680
Fax: +45 9815 1583
Email: {jni,gfp}@cpk.auc.dk

Comparison of Total Received Power and Mean Effective Gain for Mobile Handsets

Jesper Ødum Nielsen, Gert Frølund Pedersen

January 9, 2002

Abstract

This work compares different methods for performance evaluation of mobile handsets. The total radiated power (TRP) and Total Receiver Sensitivity (TRS) are compared with the more general mean effective gain (MEG) which is more realistic since it incorporates information about channel attenuation as function of direction, as well as polarization properties.

Although some similarites were found, the results show that the TRP and TRS may be misleading by many dB's compared to the MEG.

1 Introduction

When evaluating the communication performance of a mobile phone it is necessary to include the antenna, as the antenna has a large influence on the communication. This can be seen from the fact that all mobile phones fulfill the system criterion within the small tolerances allowed, but still some phones have coverage where others do not. This can be explained only by the antenna, which is not included in the type approval but of cause will be included in the real life.

In the evaluation of the communication performance of a mobile phone, the single most important parameter is the received signal power, which is the focus of this work. The received signal power depends directly on the transmitted power and on the direction and polarization at the transmitter as well as at the receiver — the antenna radiation pattern. All this comes directly from Friis' transmission law. The amount of transmitted and received power depends for any given antenna on the antenna efficiency and the matching between the antenna and the transmitter or receiver. This part can simply be measured in an anechoic room by measuring the transmitted or received power in all directions on a sphere and then integrated over the sphere. This quantity is here defined as the TRP for the transmitter case and TRS for the receiver case.

Inclusion of the direction and polarization properties of the transmitted or received power is more difficult in the case of a mobile phone due to the multipath environment where the phones typical are used.

Opposite to the case of *e.g.*, a TV antenna the signal is received from many directions and with different polarizations. In order to find the resulting received power knowledge of the distribution of the incoming power is needed as specified by [1]. The the MEG defined in [2, 3] gives the received power in the case of a scattered environment with respect to a reference antenna and will be used in this work. As discussed above, the received power depends in principle on both the antenna efficiency including the matching given by the TRP and TRS, as well as the directional and polarization properties, which is included in the MEG. In this paper the difference between the MEG and the TRP or TRS is investigated.

2 Mean Effective Gain

The signal received by a mobile handset antenna can be modeled as a linear convolution of the transmitted signal with a complex impulse response (IR) $h(\tau)$ assumed to be time-invariant.

Using that the signal received by an antenna is a weighted integration of the signal distribution in space [1], it may be verified that the IR can be written as

$$h(\tau) = \oint_S e_\theta(\Omega) D_\theta(\Omega,\tau) + e_\phi(\Omega) D_\phi(\Omega,\tau)\, d\Omega \tag{1}$$

where e_θ and e_ϕ are the complex electric field received in the θ- and ϕ-polarizations of the antenna, respectively, and where $D_\theta(\Omega,\tau)$ and $D_\phi(\Omega,\tau)$ describe the signal distribution for the two polarizations as a function of the solid angle Ω and delay τ. The integration is over the complete sphere surrounding the mobile handset. $D_\psi(\Omega,\tau)$ may be viewed as a directional IR for the ψ-polarization, where ψ is used to represent either θ or ϕ. Denoting the expectation operator by $\mathcal{E}(\cdot)$, the total received power is given by

$$\begin{aligned} P_{\text{rec}} &= \int \mathcal{E}\big(|h(\tau)|^2\big)\, d\tau \\ &= \oint |e_\theta(\Omega)|^2 Q_\theta(\Omega) + |e_\phi(\Omega)|^2 Q_\phi(\Omega)\, d\Omega \end{aligned} \tag{2}$$

where $Q_\psi(\Omega) = \int \mathcal{E}\big(|D_\psi(\Omega,\tau)|^2\big)\, d\tau$ and unit transmit power was assumed. In arriving at (2) it was used that

$$\mathcal{E}\big[D_\psi(\Omega,\tau) D_\psi^*(\Omega',\tau)\big] = \mathcal{E}\big[|D_\psi(\Omega,\tau)|^2\big]\delta(\Omega-\Omega')$$

The cross-terms $\mathcal{E}\big[D_\theta(\Omega,\tau) D_\phi^*(\Omega',\tau)\big] = 0$. These assumptions can be verified given that the phases of $D_\psi(\Omega,\tau)$ are independent for different angles and furthermore independent of the amplitude. A power density function can be defined as

$$P_\psi(\Omega) = Q_\psi(\Omega)/C_\psi \tag{3a}$$

$$C_\psi = \oint_S Q_\psi(\Omega)\, d\Omega \tag{3b}$$

C_ψ represents the power that would be recevied by an ideal ψ-polarized, isotropic antenna. Therefore, a measure of the effectiveness of the antenna is

$$\begin{aligned} \Gamma &= \frac{P_{\text{rec}}}{C_\theta + C_\phi} \\ &= \frac{\oint_S G_\theta(\Omega) Q_\theta(\Omega) + G_\phi(\Omega) Q_\phi(\Omega)\, d\Omega}{\oint_S Q_\theta(\Omega) + Q_\phi(\Omega)\, d\Omega} \end{aligned} \tag{4}$$

where $G_\psi(\Omega) = |e_\psi(\Omega)|^2$ is the gain in the ψ-polarization. The mean effective gain (MEG) quantity Γ is the ratio of actually received power to the power that would be received by two ideal, isotropic antennas. The MEG expression may be interpreted as a weighted integration of the power received from different directions, where the integration weights are determined by the handset radiation pattern.

For practical computations the surface integrals in (4) are approximated using finite summations. Expressed in spherical coordinates the integrand is assumed constant in angle intervals of size Δ_θ and Δ_ϕ, respectively, and

$$\theta_i = i \cdot \Delta_\theta \qquad \phi_j = j \cdot \Delta_\phi \tag{5a}$$

$$\Delta_\theta = \frac{\pi}{M} \qquad \Delta_\phi = \frac{2\,\pi}{N} \tag{5b}$$

with $i \in \{0,1,\ldots,M-1\}$ and $j \in \{0,1,\ldots,N-1\}$, and where θ_i is the ith spherical angle and ϕ_i is the jth azimuthal angle. Note that the sphere surface is sampled non-uniformly.

The MEG was derived above for the downlink (DL) situation, but the expressions holds for the uplink (UL) case also, except for a different interpretation of (3).[1] For the UL, C_ψ is the power that would be received at the base station if an ideal ψ-polarized isotropic antenna was used for transmission. This means that the MEG for the UL case is the power received from the device under test (DUT) as a ratio to the power that would be received if two ideal isotropic transmitter antennas were used in the same environment.

For the UL direction, Equation 4 may be seen as a weighted integration of the power transmitted by the handset antenna, where the weights

[1] The downlink is defined to be the link from the base station towards the mobile. The uplink is the link in the opposite direction.

are determined by the mobile channel in terms of $Q_\theta(\cdot)$ and $Q_\phi(\cdot)$.

Note that $e_\psi(\Omega)$ is the radiation pattern of the handset antenna in both the UL and DL cases. Also note that the UL MEG can be computed even if the directional IR is measured in the DL direction, since the channel is reciprocal.

3 Environments

Since the MEG is defined as a ratio, the absolute power level in the environment is not important for the MEG computation. Therefore only the power density function $P_\psi(\theta, \phi)$ is needed [see (3)] together with the cross polarization difference (XPD) defined as

$$\chi = 10 \cdot \log_{10}\left(\frac{C_\theta}{C_\phi}\right) \tag{6}$$

The following subsections describe five models of the environment which are used later for computing the MEG values for the measured handsets.

3.1 Rectangular Power Density

The rectangular power density function is constant versus azimuth angle, and has a rectangular shape in the elevation angle. [2] Each of the two functions are defined as

$$P_\psi(\theta, \phi) = \begin{cases} K_\psi, & |\theta - \pi/2| \le \theta_{c,\psi} \\ 0, & \text{otherwise} \end{cases} \tag{7}$$

where $0 < \theta_{c,\psi} \le \pi/2$ defines the size of the non-zero part. The constant K_ψ is chosen so that $P_\psi(\cdot)$ integrates to one.

In this work two versions of the rectangular power density model is used, one with $\chi = 0$ dB, and another with $\chi = 6$ dB.

3.2 Isotropic Power Density

The isotropic power density model results in a uniform weighting of the antenna pattern. It may be seen as a special case of the rectangular power density model with $\theta_{c,\theta} = \theta_{c,\phi} = \pi/2$ and an XPD of 0 dB.

It is noticed from (4) that for the isotropic power density function the MEG is

$$\Gamma = \frac{P_{\text{rec}}}{C_\theta + C_\phi} = \frac{P_{\text{TRP/TRS}}}{C_\theta + C_\phi} \tag{8}$$

where $P_{\text{TRP/TRS}}$ is the TRP or the TRS. Therefore, apart from a normalization the TRP or TRS may be viewed as a special case of the more general MEG.

3.3 HUT Power Density

Using data from an extensive measurement campaign the following parameterized model was found reasonable for several different propagation scenarios [4].

In this model the power distributions for the two polarizations are described by the same general expression, but with different parameters, and they are assumed to be invariant versus azimuth angle;

$$\begin{aligned} P_\psi(\theta, \phi) &= P_\psi(\theta) \\ &= \begin{cases} A_\psi \exp\left[-\dfrac{\sqrt{2}(\theta_\psi^0 - \theta)}{\sigma_\psi^+}\right], & 0 \le \theta < \theta_\psi^0 \\ A_\psi \exp\left[-\dfrac{\sqrt{2}(\theta - \theta_\psi^0)}{\sigma_\psi^-}\right], & \theta_\psi^0 \le \theta \le \pi \end{cases} \end{aligned} \tag{9}$$

where A_ψ is a constant adjusted so that (9) integrates to unit power. The remaining parameters were derived from measurements; for the outdoor to indoor propagation scenario the parameters are,

$$\begin{aligned} \theta_\theta^0 &= 90.2^\circ \quad & \sigma_\theta^- &= 5.4^\circ \quad & \sigma_\theta^+ &= 5.5^\circ \\ \theta_\phi^0 &= 90.2^\circ \quad & \sigma_\phi^- &= 8.1^\circ \quad & \sigma_\phi^+ &= 8.3^\circ \end{aligned}$$

The XPD was found to be 10.7 dB.

3.4 MBK Power Density

This model has been derived from numerous measurements of the incoming spherical power

[2] Note that in this work the elevation angle is defined as the angle from the z-axis.

density in an urban environment, where in all cases the transmitter was located outdoor and the receiver inside a four story building [5, 6] In this model the densities are seperable as follows,

$$P'_\theta(\theta,\phi) = P^\theta_\theta(\theta)P^\phi_\theta(\phi) \tag{10a}$$

$$P'_\phi(\theta,\phi) = P^\theta_\phi(\theta)P^\phi_\phi(\phi) \tag{10b}$$

with the θ and ϕ parts defined as

$$P^\theta_\theta(\theta) = \frac{s^2_{\theta\theta}}{s^2_{\theta\theta}+\cos^2(\theta)} \tag{11}$$

$$P^\phi_\theta(\phi) = \begin{cases} \dfrac{s^2_{\theta\phi}}{s^2_{\theta\phi}+\sin^2(\phi')}, & |\phi'| \le \pi/2 \\ a_{\theta 0}, & |\phi'| > \pi/2 \end{cases} \tag{12}$$

$$P^\theta_\phi(\theta) = \frac{s^2_{\phi\theta}}{s^2_{\phi\theta}+\cos^2(\theta)} \tag{13}$$

$$P^\phi_\phi(\phi) = \begin{cases} \dfrac{s^2_{\phi\phi}}{s^2_{\phi\phi}+\sin^2(\phi')}, & |\phi'| \le \pi/2 \\ a_{\phi 0} - b_\phi|\phi'|, & |\phi'| > \pi/2 \end{cases} \tag{14}$$

For convenience, this model defines the azimut angle as

$$\phi' = \begin{cases} \phi, & 0 \le \phi \le \pi \\ \phi - 2\,\pi, & \pi < \phi < 2\,\pi \end{cases}$$

where ϕ is the azimuth angle used elsewhere in this work.

In [5] the following parameters are provided for the model

$$s_{\theta\theta} = 0.29 \quad s_{\theta\phi} = 1.06 \quad a_{\theta 0} = 0.16$$
$$s_{\phi\theta} = 0.44 \quad s_{\phi\phi} = 1.18 \quad a_{\phi 0} = 0.70 \quad b_\phi = 0.11$$

These parameters were obtained from a least squares fit of the model to a mean power density obtained from a large collection of measurements. The XPD for the mean power density was found to be 5.5 dB. Note that $P'_\psi(\cdot)$ in (10) generally does not integrate to one and must be normalized.

4 Handset Antenna Radiation Pattern Measurements

The purpose of the measurements is to obtain the radiation pattern in all directions and both polarizations both for the UL and the DL. To measure the radiation patterns correctly no changes can be made to the phone as, *e.g.*, adding a coaxial cable, because this will change the radiation pattern by the coupling to the external cable [7]. Further, only by including the transmitter (and receiver) in the phone the true absolute value (in dBm) can be obtained as influence from the mismatch is taken into account, *e.g.* load-pull from the power amplifier.

Figure 1: Phantom being mounted on the pedestal.

To measure the radiation patterns of the phones a setup in the anechoic room at Aalborg university including a GSM basestation emulator was used, see Figure 1. The anechoic room is 10 by 7 by 7 meters and equipped with absorbers to allow reflection free measurements in the frequency range of mobile phones. A block diagram of the setup is shown in Figure 2. The Phone Under Test (PUT) is mounted on the pedestal capable of moving in two axes to allow measurements in all directions. The probe antenna is

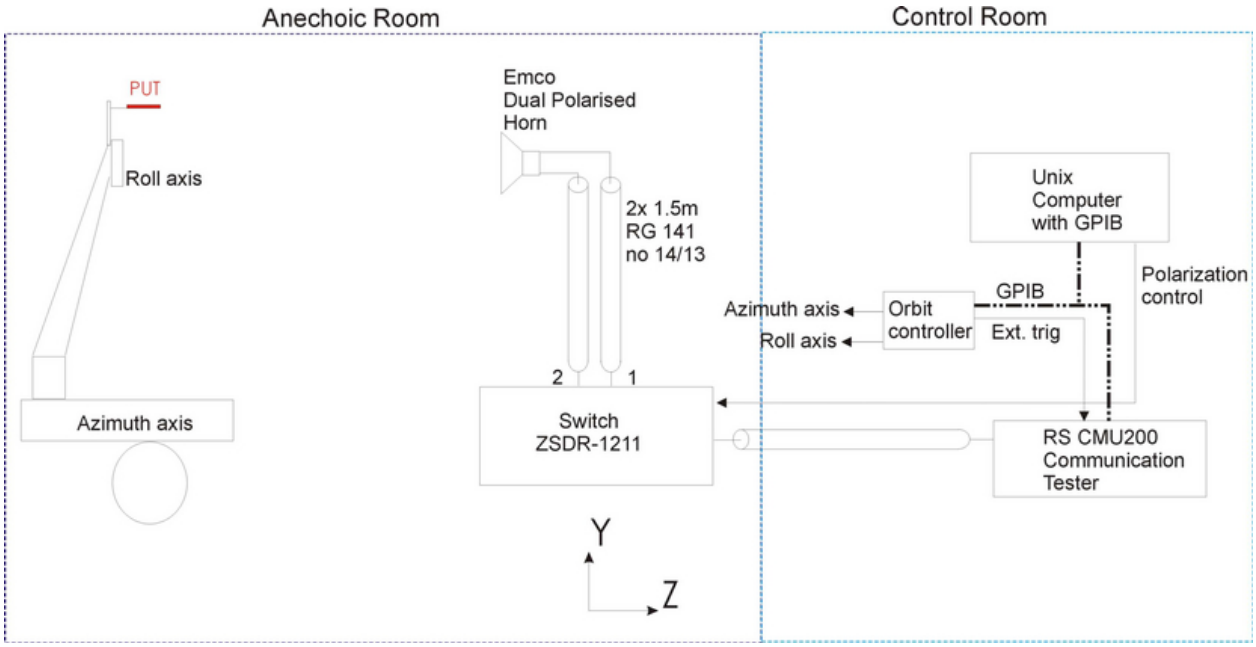

Figure 2: Block diagram of the radiation pattern measurement system.

fixed some 5.5 meters from the PUT. The measuring probe is dual polarized and one polarization at a time is both transmitting and receiving as a normal basestation. The measurement is automated and controlled by a computer via the standard GPIB interface (IEEE 488).

The procedure of a measurement starts with the basestation transmitting on its broadcast channel, the phone is searching for a broadcast channel and when it finds the broadcast channel, the phone locks to it and the basestation make an alert to the phone. When the phone alerts, the operator answers the call and a 'normal' speech connection between the base and the phone is established. The phone is then mounted on the pedestal at the rotation centre after which the controlling program starts the measurement. The program rotates the pedestal to the first position and first polarization, the basestation measures the received power (*i.e.*, the UL power), waits some 1.5 seconds (corresponding to 3 SAACH frames in GSM) and gets the measured signal strength from the phone (the DL power). Next, the controlling program changes the polarization and measures again both UL and DL power levels, and finally the phone is rotated to the next point for measurement.

When all points on the sphere are measured the controlling program moves to the point and polarization with the highest reported DL power and starts to make a scan of how linear the phone can measure the power. This is done by changing the power transmitted by the basestation from the maximum power in steps of 0.25 dB down to the level where the phone measures RxLev = 0 (corresponding to -110 dBm). The measurement of linearity can then be used to compensate for the possible inaccuracy in power measurements in the phone.

Some examples of the spherical radiation patterns are shown in Figure 3.

To include the influence of the user, measurements including a phantom torso mounted at the pedestal were made (Figure 1). The phantom is filled with a brain simulating liquid [8]. The phone is attached to the left side of the phantom with the earpiece at the position of the phantom's ear, and the phone bottom as close to the mouth as possible. For this position the phone

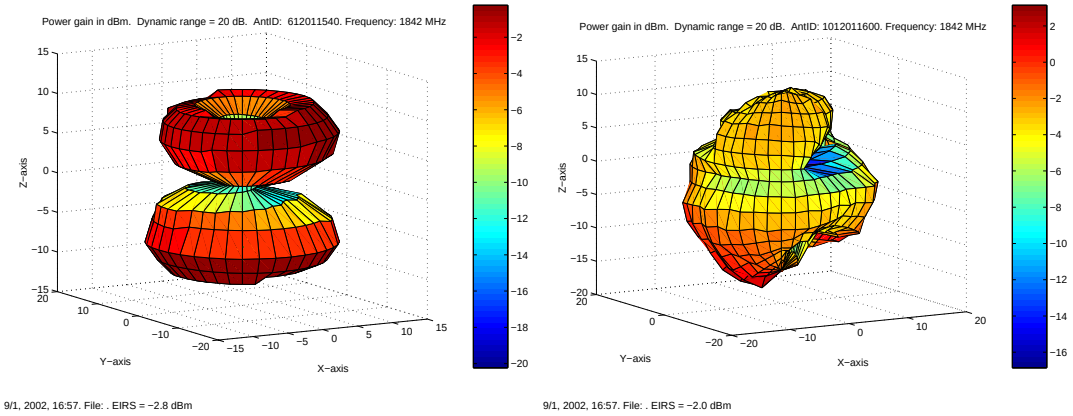

Figure 3: Measured radiation pattern for handset with retractable antenna (left), and radiation pattern for small handset (right).

angle with respect to vertical is some 45°, see Figure 4.

Four GSM handsets were used which are commercially available and represents the most important handset types used today. Handset A and B are large handsets with external and internal antennas, respectively. Handset C and D are small handsets with internal and external antennas, respectively. Here 'small' handsets are among the smallest handsets available today, about 10 cm by 4.5 cm, and the 'large' handsets are about 13 cm by 4.5 cm.

In addition some measurements were made with a substitute antenna for handset D. This antenna is a retractable whip antenna combined with a helix. Measurements with this antenna are labelled handset E (whip) and handset F (helix).

All the radiation patterns were measured using a angle increment of 10° in both azimuth and elevation angle. GSM channel 698 was used in all cases.

Figure 4: Phantom with handset mounted.

5 MEG Computations

Each handset is measured in the anechoic chamber with the long axis of the handset oriented along the z-axis and the handset top towards the positive direction. The front of the handset (keypad side) is facing the negative y-axis, so that the "width" of the handset is along the x-axis with the right hand side towards the positive part of the axis.

The MEG is computed using different rotations of the handset antenna radiation patterns. Each combination of the following angles are used

$$\mu \in \{0^\circ, 15^\circ, 30^\circ, \ldots, 345^\circ\} \tag{15a}$$

$$\lambda \in \{0^\circ, 15^\circ, 30^\circ, 45^\circ, 60^\circ, 300^\circ, 315^\circ, 330^\circ, 345^\circ\} \tag{15b}$$

where μ and λ are the rotation angles about the z-axis and the x-axis, respectively. The rotation is carried out first about the x-axis then about the z-axis.

Since the grid of measurement points is not preserved in the rotation it is necessary to intro-

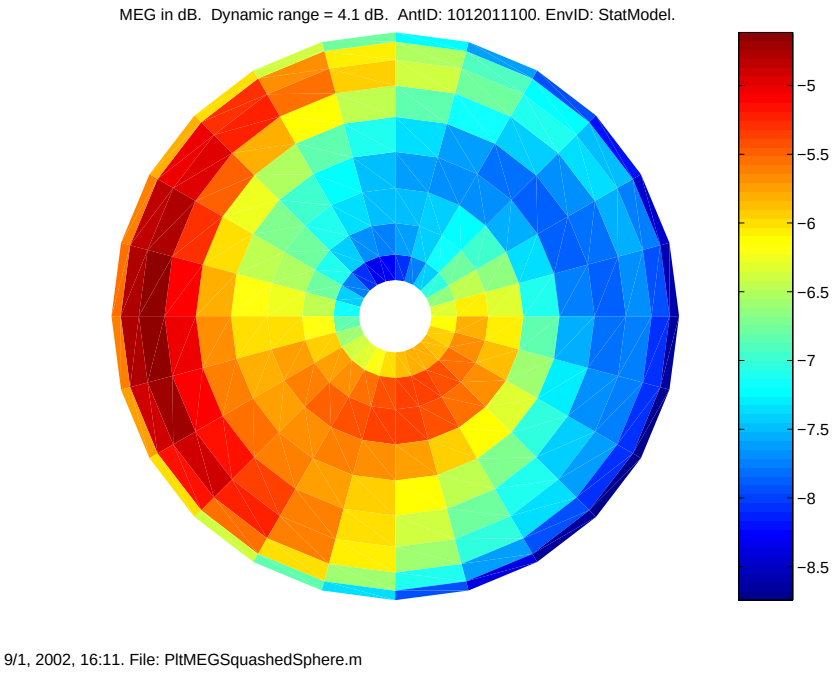

Figure 5: MEG values for handset B in free space, computed using the MBK model of the environment for the DL.

duce interpolation. A standard two dimensional linear interpolation was used.

For each combination of the rotation angles in (15) the MEG is computed, resulting in a set of MEG values for each handset measurement in a given environment. An example of the MEG values computed for handset A is shown in Figure 5. In this figure the MEG values are shown using the color code given in the bar on the right. Each polygon in the plot represents one combination of azimuthal and elevation rotation angle.

6 MEG Dependence on Environment

In Figure 6 and 7 the MEG results for the free space case are shown for the DL and UL, respectively, while Figure 8 and 9 show the results for the measurements including the phantom.

In the figures the minimum and maximum values of the computed MEG values are shown as the endpoints of a vertical line, one line for each handset. Also shown on each line is the mean value (shown with '$\times$') and a MEG value for a specific rotation, see later, marked with '$\square$'.

The results are presented in groups, one for each of the environments defined in Section 3.

Comparing the results obtained with the isotropic model with those obtained using the rectangular window model (XPD of 0 dB) it is noticed that the results are very similar. The mean values are roughly identical, which is expected since the rectangular window covering the θ-angles $[45°; 135°]$ covers about 71% of the surface area of the sphere. Hence, most of the power will be included and as the XPD is zero no weighting is introduced. Therefore the results will be close to the ones obtained with the isotropic environment.

Because the measured radiation pattern is rotated up to 60° in elevation angle some variation in the MEG values are observed for the rectangular window model, but only small changes are noticed compared to the changes seen with the two environment model derived from measurements. The rectangular window model with an XPD of 6 dB causes more changes, but the re-

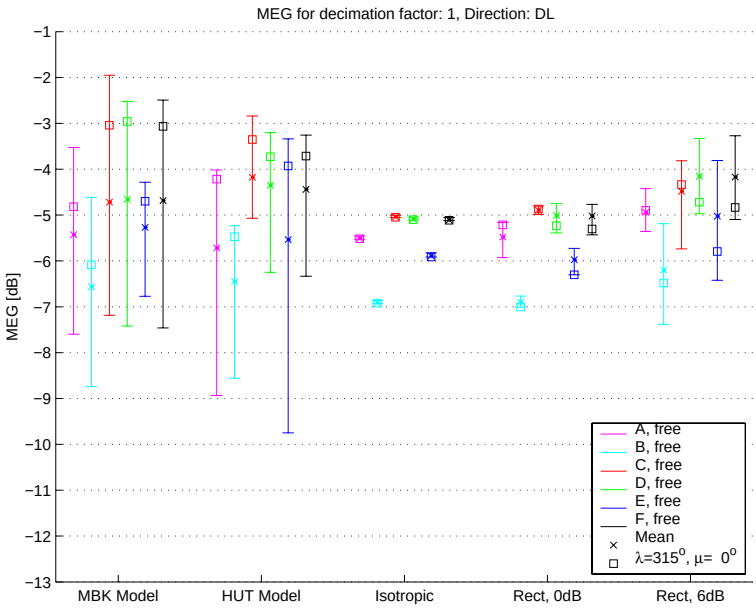

Figure 6: MEG for free space conditions in the DL direction. The minimum and maximum values are shown as error bars.

sults are still far from to those obtained with the HUT and MBK models.

Although the results obtained with the MBK model and the HUT model have some similarities, it is also clear that there are significant differences in some cases. For example for handset E in the free space case the two models result in a MEG variation of about 2.5 dB and 6.4 dB for the MBK and HUT model in the DL direction, respectively, and about 3.1 dB and 7.9 dB for the UL direction.

Regarding the mean MEG values, Table 1 and 2 show the differences in the mean MEG values obtained with the various environment models compared to the isotropic case. For the free space case (Table 1) all differences are within the range -0.2 dB up to 1 dB.

The mean values are also quite small with the phantom in case of the the rectangular window model with an XPD of 0 dB, where all differences are smaller than 0.4 dB. However, for the other models larger differneces are found. In particular the HUT model results in differences from -2.8 dB up to 0.8 dB.

Larger differences are expected for phantom measurements and the non-isotropic environment models as compared to the corresponding free space measurements. The phantom blocks some of the power and effectively makes the radiation patterns more directive than the free space patterns. This casuses more changes in the MEG when the handset is rotated and the environment model is non-isotropic.

It is important to realize that even if the mean values are identical for two different models of the environment this does not imply that the MEG values obtained with the two models are identical for a specific rotation of the radiation pattern.

For the free space an example is the rotation of the measured radiation pattern with $\lambda = 315°$ and $\mu = 0°$, corresponding to a tilt angle of 45° in typical talk position. The MEG values obtained with these rotations are shown on the vertical lines in Figure 6–7 with a '□'. It is clearly not possible to predict the MEG values shown with the □-marks from the mean values.

The same is also true for the phantom measurements. For the phantom measurements $\lambda = 0°$ and $\mu = 0°$ is used since the handset is already mounted at an angle of 45° on the phantom.

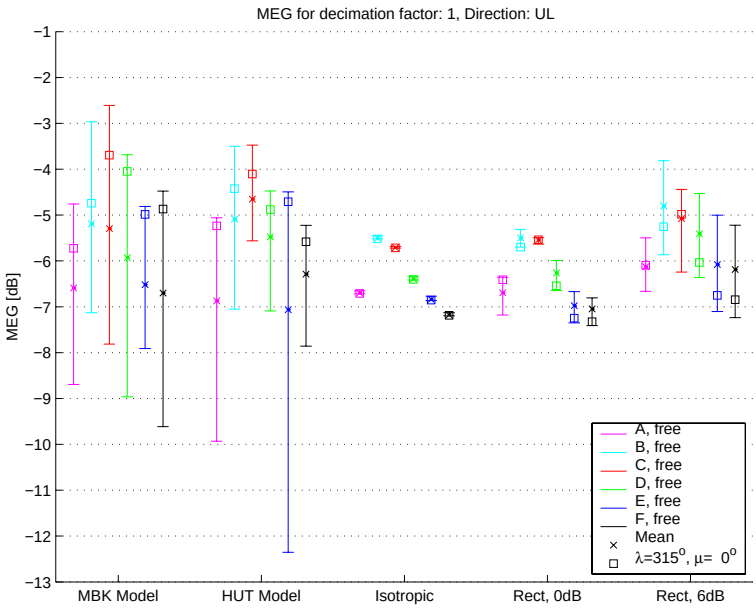

Figure 7: MEG for free space conditions in the UL direction. The minimum and maximum values are shown as error bars.

	DL						UL					
Environment	*A*	*B*	*C*	*D*	*E*	*F*	*A*	*B*	*C*	*D*	*E*	*F*
MBK	0.1	0.3	0.3	0.4	0.6	0.4	0.1	0.3	0.4	0.5	0.3	0.5
HUT	−0.2	0.5	0.9	0.7	0.4	0.7	−0.2	0.4	1.1	0.9	−0.2	0.9
Isotropic	0.0	0.0	0.0	0.0	0.0	0.0	0.0	0.0	0.0	0.0	0.0	0.0
Rect, 0 dB	0.0	0.0	0.1	0.1	−0.1	0.1	0.0	0.0	0.2	0.1	−0.1	0.1
Rect, 6 dB	0.6	0.7	0.6	0.9	0.9	0.9	0.6	0.7	0.6	1.0	0.8	1.0

Table 1: Difference in mean MEG values with the isotropic case as reference, all values are in dB and for the free space case.

7 MEG Dependence on Spherical Sampling Density

The goal in this section is to study the effect of reducing the number of samples in the spherical radiation pattern, and thus the total measurement time. However, by reducing the number of samples some errors are introduced which is a combination of errors due to insufficient sampling of the antenna radiation pattern and errors in the linear interpolation performed during the rotation of the radiation pattern.

Originally the antenna radiation patterns were measured with an angle increment of $\Delta_\theta = \Delta_\phi = \Delta_\psi = 10°$. By omitting samples from the measurements, the following values of angle increments were tested: $\Delta'_\psi \in \{10°, 20°, 30°, 60°\}$. Apart from the sampling density, the MEG was computed in the same way as for the results presented in Section 6.

In order to limit the amount of data, results are only shown for one specific rotation of the handset — the same rotation as mentioned above in Section 6, *i.e.*, $\lambda = 315°$ and $\mu = 0°$ for free space measurements, and $\lambda = 0°$ and $\mu = 0°$ for the phantom measurements.

Table 3 and 4 show the results the isotropic environment model as well as the MBK model

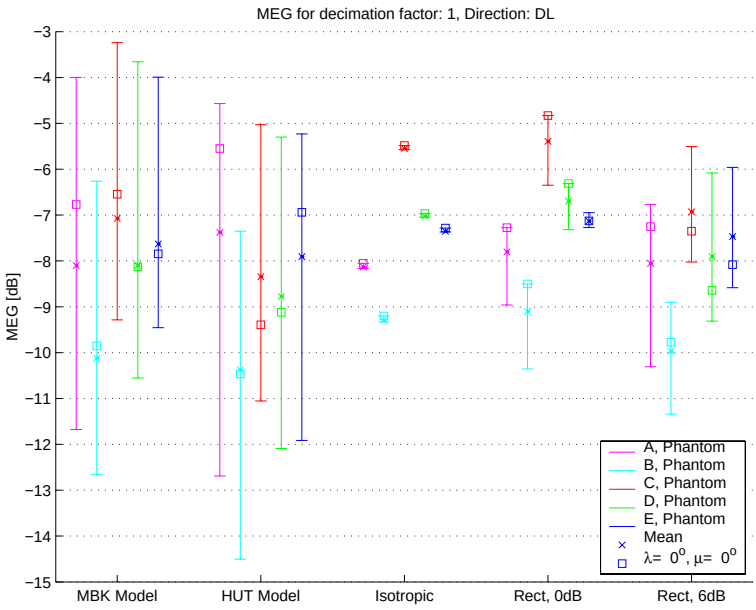

Figure 8: MEG for handset including phantom in the DL direction. The minimum and maximum values are shown as error bars.

	DL					UL				
Environment	*A*	*B*	*C*	*D*	*E*	*A*	*B*	*C*	*D*	*E*
MBK	0.0	−0.8	−1.5	−1.1	−0.3	−0.0	−1.0	−1.4	−1.2	−0.5
HUT	0.8	−1.1	−2.8	−1.7	−0.6	0.7	−1.6	−2.6	−1.9	−1.0
Isotropic	0.0	0.0	0.0	0.0	0.0	0.0	0.0	0.0	0.0	0.0
Rect, 0 dB	0.3	0.2	0.2	0.3	0.2	0.4	0.2	0.1	0.3	0.2
Rect, 6 dB	0.1	−0.7	−1.4	−0.9	−0.1	0.1	−0.8	−1.3	−1.0	−0.4

Table 2: Difference in mean MEG values with the isotropic case as reference, all values are in dB and for the phantom case.

in the UL case. All values have been normalized to the values at $\Delta_\psi = 10°$

As expected, the results in both of the tables indicate a generally increasing normalized error for increasing values of Δ'_ψ. For $\Delta'_\psi = 20°$ and $\Delta'_\psi = 30°$ the errors are in the range −0.3 dB to 0.0 dB for the free space case and −0.3 dB to 0.2 dB for the phantom measurements, and thus quite small compared to the changes in MEG observed in Section 6.

For $\Delta'_\psi = 60°$ the errors are somewhat larger, up to ±0.6 dB for the free space case, and between −1.3 dB and 1.1 dB for the phantom case

8 Conclusion

The difference in TRP (and TRS) for the 5 radically different mobile phones is only some 3 dB, which of course from a power consumption point of view is significant, but it is low compared to the variation in real use, as expressed by the MEG. By not including the MEG obtained by using realistic models of the incoming power, the results of a validation or accreditation is questionable.

To obtain the correct MEG values the actually user position is important as well as a realistic model of the incoming power. The model of the incoming power may vary significantly from one

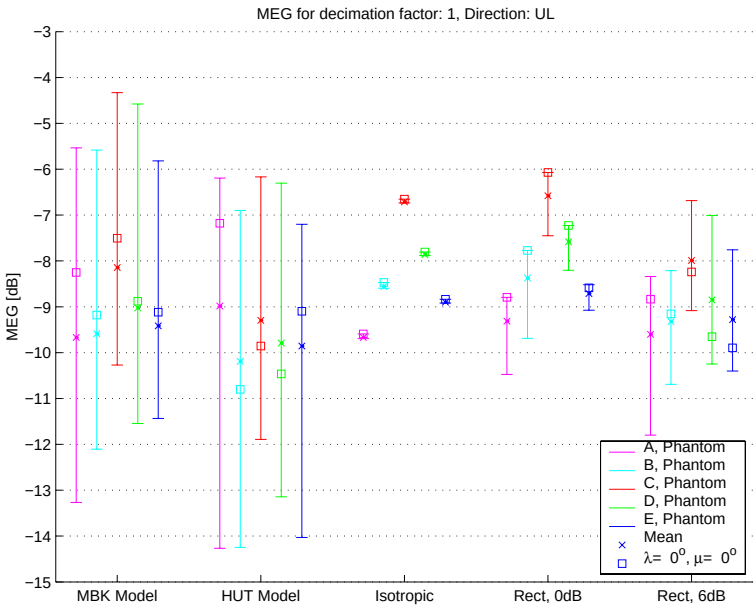

Figure 9: MEG for handset including phantom in the UL direction. The minimum and maximum values are shown as error bars.

	Isotropic						MBK power density					
Δ_ψ	A	B	C	D	E	F	A	B	C	D	E	F
10°	0.0	0.0	0.0	0.0	0.0	0.0	0.0	0.0	0.0	0.0	0.0	0.0
20°	−0.1	−0.1	0.0	−0.1	−0.1	0.0	0.0	0.0	0.0	0.0	0.0	0.0
30°	−0.2	−0.2	0.0	−0.0	−0.1	0.0	−0.1	0.0	−0.1	−0.2	−0.3	−0.2
60°	0.6	0.3	0.0	0.1	0.8	0.1	−0.1	−0.5	−1.0	−0.6	0.2	−0.6

Table 3: MEG for different sampling densities relative to MEG for $\Delta_\psi = 10°$. Free space measurements rotated with $\lambda = 315°$ and $\mu = 0°$.

environment to another and it may be necessary to define several models to cover the different environments similar to *e.g.*, the channel models defined for the mobile systems.

The results show not only that TRP (and TRS) is inaccurate and that the radiation pattern of the phone is important but also that the radiation pattern can be measured with a significantly reduced sampling compared to the basic sampling of 10°.

References

[1] William C. Jakes. *Microwave Mobile Communications*. IEEE Press, 1974.

[2] Jørgen Bach Andersen and Flemming Hansen. Antennas for VHF/UHF personal radio: A theoretical and experimental study of characteristics and performance. *IEEE Transactions on Vehicular Technology*, 26(4):349–357, November 1977.

[3] Tokio Taga. Analysis for mean effective gain of mobile antennas in land mobile radio environments. *IEEE Transactions on Vehicular Technology*, 39(2):117–131, May 1990.

[4] Kimmo Kalliola, Kati Sulonen, Heikki Laitinen, Outi Kivekäs, Joonas Krogerus, and Pertti Vainikainen. Angular power distrubtion and mean effective gain of mobile an-

	Isotropic					MBK power density				
Δ_ψ	A	B	C	D	E	A	B	C	D	E
10°	0.0	0.0	0.0	0.0	0.0	0.0	0.0	0.0	0.0	0.0
20°	0.1	0.1	0.0	0.1	0.1	0.0	0.2	0.1	0.2	0.2
30°	−0.1	−0.0	−0.1	0.0	−0.1	0.2	−0.3	−0.3	−0.2	−0.1
60°	0.2	1.1	0.6	0.6	0.3	−1.3	1.1	0.9	0.7	−0.1

Table 4: MEG for different sampling densities relative to MEG for $\Delta_\psi = 10°$. Free space measurements rotated with $\lambda = 315°$ and $\mu = 0°$.

tenna in different propagation environments. Technical report, Helsinki University of Technology Radio Laboratory Publications, Report S 249, 2001.

[5] Mikael B. Knudsen and Gert F. Pedersen. Spherical outdoor to indoor power spectrum model at the mobile terminal. Accepted for publication in "IEEE Journal on Selected Areas in Communications".

[6] Mikael Bergholz Knudsen. *Antenna Systems for Handsets*. PhD thesis, Center for PersonKommunikation, Aalborg University, September 2001. Can be reached at http://home1.stofanet.dk/grenen7.

[7] Wim A. Th. Kotterman, G. F. Pedersen, and P. Eggers. Cable-less measurement set-up for wireless handheld terminals. In *Personal, Indoor and Mobile Radio Communications conference, PIMRC 2001*, pages B112–B116, September 2001.

[8] Schmid & Partner, http://www.speag.com/. Generic torso phantom, v.3.6.